Journal of *Marine Science and Engineering*

MDPI

Article

Development and Application of an Integrated System for the Detection and Prediction of Harmful Algal Blooms in Korea

Donhyug Kang [1], Byoung Kweon Kim [2], Seung Won Jung [3], Seung Ho Baek [4], Jin-Yong Choi [5], Hong-Yeon Cho [6], Sun-Ju Lee [7] and Hansoo Kim [1,*]

1 Marine Domain and Security Research Department, Korea Institute of Ocean Science & Technology (KIOST), Busan 49111, Republic of Korea; dhkang@kiost.ac.kr
2 Syscore Inc., Yongin 16897, Republic of Korea; bkkim@syscore.co.kr
3 South Sea Research Institute, Korea Institute of Ocean Science & Technology (KIOST), Geoje 53201, Republic of Korea; diatoms@kiost.ac.kr
4 Ecological Risk Research Department, Korea Institute of Ocean Science & Technology (KIOST), Geoje 53201, Republic of Korea; baeksh@kiost.ac.kr
5 Coastal Disaster and Safety Research Department, Korea Institute of Ocean Science & Technology (KIOST), Busan 49111, Republic of Korea; dol76@kiost.ac.kr
6 Marine Bigdata and A.I. Center, Korea Institute of Ocean Science & Technology (KIOST), Busan 49111, Republic of Korea; hycho@kiost.ac.kr
7 Korea Ocean Satellite Center, Korea Institute of Ocean Science & Technology (KIOST), Busan 49111, Republic of Korea; sunjulee@kiost.ac.kr
* Correspondence: hskim@kiost.ac.kr; Tel.: +82-51-664-3654

Abstract: Harmful algal blooms (HABs) are types of phytoplankton overgrowth that adversely affect marine ecosystems and aquaculture resources. One such HAB species, *Cochlodinium polykrikoides*, occurs irregularly and causes significant damage to the aquaculture industry along the coastal regions of Korea. In this study, we developed and implemented an integrated system to detect and predict HAB occurrences in real time. This system comprises four main components: (1) a real-time detection system utilizing acoustic sensing, ocean weather, water temperature, salinity, and chlorophyll, satellite images, genetic analysis, and optics; (2) a prediction model system based on current and tidal, HAB occurrence, and HAB movement and diffusion models; (3) an additional data based on HAB information of sampling data and HAB information of GPS data, and (4) an integrated information system utilizing data storage servers and a visualization platform. We applied and assessed the efficiency of this integrated system in the South Sea of Korea from 2017 to 2019. Particularly, HABs occurred significantly in 2019, and the system demonstrated the feasibility of detection and prediction under field conditions. Implementing a more advanced integrated detection and prediction system in the field is anticipated to minimize the damage caused by irregular HAB occurrences every year.

Keywords: integrated system; detection and prediction; harmful algal bloom; *Cochlodinium polykrikoides*

Citation: Kang, D.; Kim, B.K.; Jung, S.W.; Baek, S.H.; Choi, J.-Y.; Cho, H.-Y.; Lee, S.-J.; Kim, H. Development and Application of an Integrated System for the Detection and Prediction of Harmful Algal Blooms in Korea. *J. Mar. Sci. Eng.* **2023**, *11*, 2207. https://doi.org/10.3390/jmse11122207

Academic Editor: Hesham M. El-Askary

Received: 26 September 2023
Revised: 3 November 2023
Accepted: 18 November 2023
Published: 21 November 2023

1. Introduction

Harmful algal blooms (HABs) are one of the primary causes of the degradation of living marine resources [1]. Such blooms continue to occur irregularly and cause severe damage, particularly in the coastal oceans of Korea, Japan, Taiwan, and other southeast Asian countries [2,3]. HABs can directly or indirectly affect the fishing industry, marine ecosystems, local economies, and tourism through the loss of observation personnel and costs [4,5]. The ichthyotoxic, unarmored dinoflagellate *Cochlodinium polykrikoides* is one of the most common HABs implicated in mass fish mortality events worldwide [1,2,6].

Tidal effects can elicit unexpected, rapid HAB growth and accumulation. Therefore, efforts have been made to develop monitoring tools and techniques to provide early warnings for HAB formation. To minimize HAB-induced damage, early observation of their

formation is necessary [4,7,8]. Therefore, methods for HAB observation and monitoring are actively being explored.

Research on HAB detection in Korea has traditionally relied on in-situ observations. Water sampling is conducted using ships and researchers, with daily results made publicly available. Alternatively, remote sensing techniques employing satellites to measure chlorophyll-a (Chl-a) concentrations have been employed. This method allows for rapid monitoring over a wide area and provides scientific data essential for efficient control [9–12]. In Korea, HAB detection using Chl-a concentration images primarily relies on ocean color sensors such as the Geostationary Ocean Color Imager (GOCI), SeaWiFS, MERIS, MODIS, and OLCI. These sensors are designed to assess ocean quality [13–16]. However, this method has a low spatial resolution (250–1000 m) and is affected by weather conditions (e.g., typhoons, clouds, rain). Molecular tools, such as real-time qPCR gene analysis, have also been proposed as rapid HAB detection methods [17]; qPCR can detect low concentrations of HAB species. However, this method requires specialists trained in laboratory settings. Several devices have been developed and deployed to overcome these methodological shortcomings for real-time HAB detection and monitoring. Two of these instruments include the environmental sample processor, which automatically collects and analyzes water samples for the DNA of HAB, and the imaging FlowCytobot. This automated underwater microscope generates high-resolution micrographs of particles suspended in water [18,19]. However, these instruments are expensive to install and maintain. Recently, hydroacoustic technology has been demonstrated to be a low-cost and highly efficient method for continuously measuring HABs [20,21].

HAB occurrence prediction depends mainly on numerical models, which forecast the spatiotemporal extent of HAB events. Some models developed for numerical ocean modeling include the finite volume coastal ocean model (FVCOM), environmental fluid dynamics code (EFDC), and Princeton Ocean Model (POM) [22,23]. Despite their increasing accuracy of HAB forecasts, these models introduce uncertainty in all predictions owing to the oceanic environment and ecological characteristics of phytoplankton. The accuracy of methods for predicting HAB movement and spread needs improvement [24].

Ocean observation data and modeling results are typically large-volume, multi-source, and multi-dimensional. Generally, understanding, analysis, and utilization of these complex datasets are difficult for end users. Collecting these datasets into a single system and visualizing them in a geospatial context would significantly improve the understanding and management of HABs. Recent progress in the web-based geographic information system (GIS) technology has provided excellent opportunities to achieve this goal. Recently, Tian and Huang developed a HAB monitoring and forecasting system using a web-based GIS that provides a graphic interface for users and managers to view real-time in-situ measurements and remote sensing maps to explore and obtain numerical model forecasts and early warning information [25].

HABs have occurred irregularly in Korean coastal oceans since the 1990s [26,27]. In Korea, economic losses due to HABs were estimated to be USD 70 million in 1995, USD 4–18.6 million per year in 2000–2003 and 2007, and USD 24.7 million in 2013 [28–30]. Research on their detection and prediction is necessary to minimize damage caused by HAB on the Korean coastal oceans.

In this study, we aimed to establish an integrated detection and prediction system for HABs to provide advanced information on such blooms and minimize the ecological damage they irregularly cause yearly. To this end, various real-time detection tools, such as acoustics, ocean weather and environment, and satellites that detect HABs, were operated. HAB movement and diffusion prediction models were developed and applied based on the oceanographic numerical model (Korea Operational Oceanographic System, KOOS). Finally, an integrated system for obtaining real-time information was developed by combining technologies for detecting and predicting HAB occurrence. This paper presents the results of establishing and operating an integrated system in the South Sea of Korea.

2. Methodology

2.1. Study Area

In Korea, *C. polykrikoides* predominantly appears along the southern coast during the summer [2,3]. This region, particularly the South Sea coast, hosts numerous commercial fish farms, leading to annual economic losses due to HABs [26–30]. Before selecting the measurement area, we analyzed data on HAB occurrence areas obtained from Korean public institutions, such as the National Institute of Fisheries Science (NIFS), over the past two decades [5]. Based on this analysis, we selected the study area located on the southern coast of Korea, encompassing Tongyeong, Yeosu, and Geoje. These areas are consistently affected by HAB-induced damage every year (Figure 1). The study area has depths ranging from approximately 10 m to 30 m and is densely populated with various commercial fish farms.

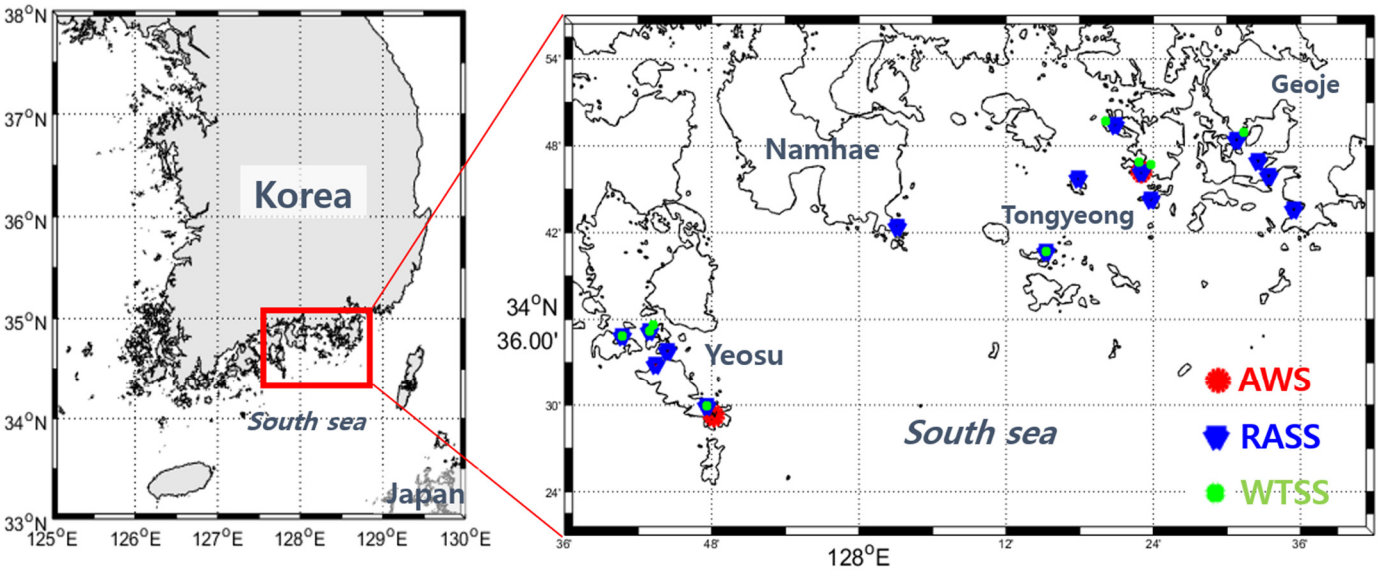

Figure 1. Installation stations of the automatic weather system (AWS), red tide acoustic sensing system (RASS), and water temperature sensing system (WTSS) in the South Sea of Korea (red circle: AWS; blue triangle: RASS; green circle: WTSS).

The coastal and offshore oceans where fish farms are concentrated were selected to apply the HAB detection systems in the oceans. The automatic weather system (AWS) was installed and operated at two stations, the red tide acoustic sensing system (RASS) (SC-RTC100, Syscore Inc., Yongin, Korea) was installed and operated at 15 stations, and the wireless temperature sensing system (WTSS) (SC-WT100, Syscore Inc., Yongin, Korea) was installed and operated at nine stations. The water depth of the sites where the HAB detection systems were installed and operated was between 10 m and 35 m. Many private fish farms are concentrated in the oceans, as islands or bays surround them. Because acoustics and marine environmental data must be recorded at critical stations to efficiently observe HABs in this environment, a real-time HAB detection system was installed and operated by conducting field surveys and selecting a specific cage farm where HABs frequently occur.

2.2. System Framework

2.2.1. System Architecture

The developed Korea Ocean REd tide Detection and prediction (KORED) system integrates various essential technologies, such as real-time detection in the ocean and predictive analysis of HAB movement and diffusions. It aims to establish an integrated information support system for fishermen, fishing villages, and local governments. The KORED system

amalgamates diverse elemental technologies frequently employed in various HAB research fields at KIOST. This integrated KORED system comprises the following four components:

(1) Real-time HAB detection systems: ocean weather (AWS), acoustic (RASS), ocean environment (water temperature, salinity, and chlorophyll-a, RASS & WTSS), satellite imagery (Geostationary Ocean Color Imager, GOCI), sampling, genetic analysis, and optical data;
(2) Prediction systems based on the HAB model: KOOS, HAB occurrence, and HAB movement and diffusion models;
(3) Additional data: HAB information of sampling data from NIFS and HAB information of GPS data from our developed application;
(4) Integrated information system: data storage server, file transfer protocol (FTP) server, and visualization system.

The integrated information system for the obtained detection and prediction data was implemented to provide information to NIFS research institutes and fishing villages/fishermen. A configuration diagram of the system is shown in Figure 2, and the variables, resolution, sites, data period, and data format of the integrated HAB detection, prediction, and information system are shown in Table 1.

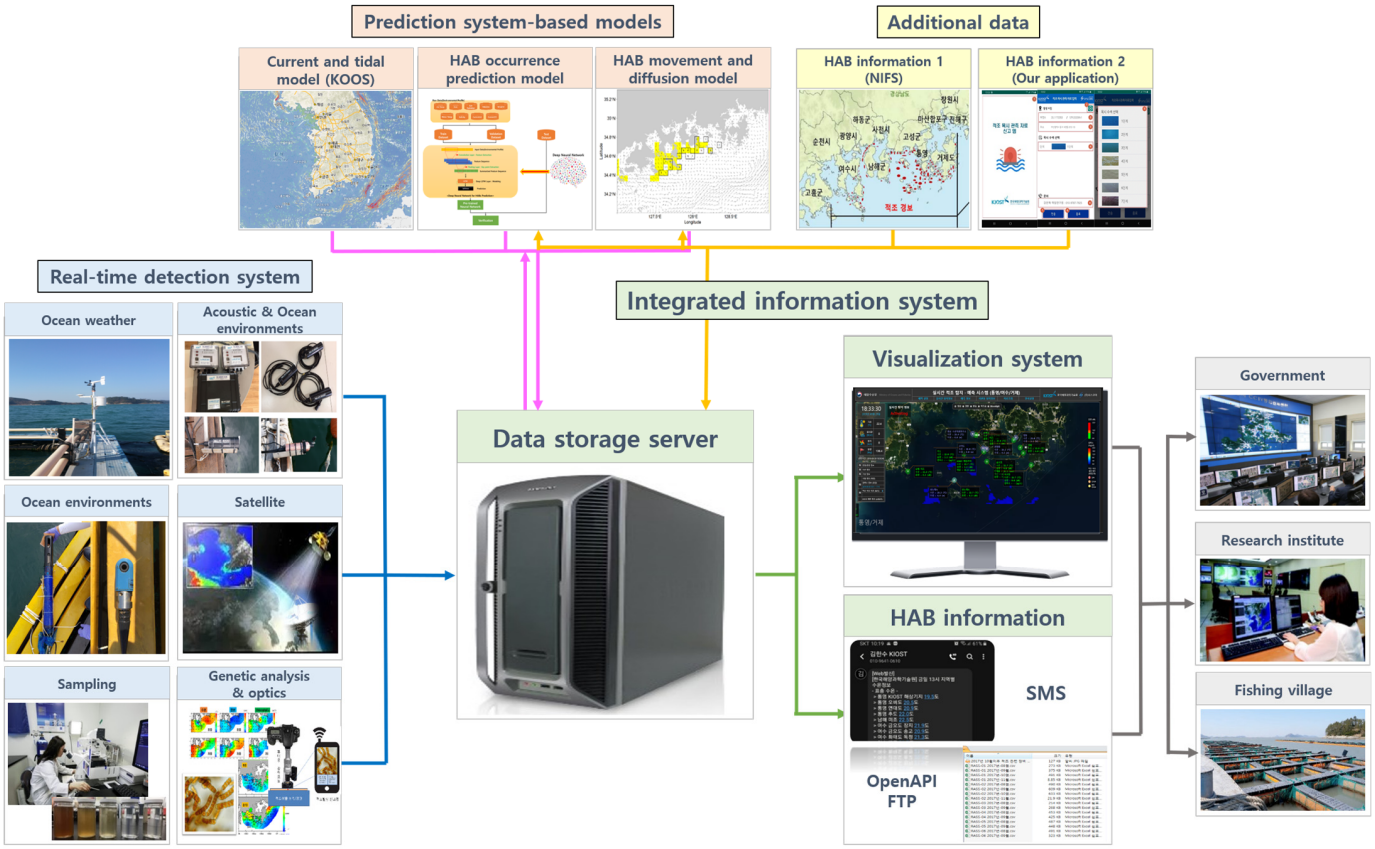

Figure 2. Schematic of real-time HAB detection, prediction (model), and integrated information systems (called the KORED system).

Table 1. Variables, resolution, sites, data period, and data format of integrated HAB detection, prediction, sampling data, and information systems (T: Tongyeong, G: Geoje, Y: Yeosu, S: South Sea of Korea).

System	Variable	Data	Resolution	Site	Data Period	Data Format
Detection system	Ocean weather (AWS)	Date, time, GPS, air temperature, solar radiation, wind speed, and wind direction data	Point (Station)	T, G, Y	10 min (Continuous)	csv
	Acoustic and ocean environment (RASS, WTSS)	(1) RASS: Date, time, GPS, acoustic intensity, water temperature, and salinity (Some stations: Chl-a, dissolved oxygen (DO), and pH (2) WTSS: Date, time, GPS, water temperature, and water pressure	Point (Station)	T, G, Y	10 min (Continuous)	csv
	Satellite (GOCI)	Date, time, GPS, and chlorophyll-a concentration (RBR)	500 m	T, G, Y	1 h (8 times/daytime)	netCDF
			500 m	S	1 h (8 times/daytime)	netCDF
Prediction system (model)	Korea operational oceanographic system (KOOS) model	(1) Marine meteorological information: Date, time, GPS, wind, and atmospheric pressure	150 m	T, G, Y	1 time (72 h/1 h)	netCDF
		(2) Marine environmental information: Date, time, GPS, waves, tides, currents, ocean currents, water temperature, and salinity per depth	300 m	S	1 time (72 h/1 h)	netCDF
	HAB occurrence model	Date, time, GPS, and presence or absence of HAB	5 km	T, G, Y	1 time (after 72 h)	csv
	HAB movement and diffusion model	Date, time, GPS, and level of HAB	300 m	S	1 time (72 h/1 h)	netCDF
Additional data (others)	HAB information 1 (from NIFS)	Date, time, GPS, and *C. polykrikoides* population	Point	T, G, Y, S	1 day	netCDF
	HAB information 2 (from our application)	Date, time, GPS, and *C. polykrikoides* population	Point	T, G, Y, S	1 day	csv
Information system	FTP server	-			Real-time	
	Integrated visualization system	-		T, G, Y, S	Real-time	Web-based

2.2.2. Real-Time Detection System

The RASS, the HAB detection system, detects HABs using sound waves based on sound scattering theory [20,21]. Real-time measurements of sound intensity and water temperature reflected from phytoplankton once every 10 min through a long-range communication system based on IoT technology (LoRa, SK Telecom Inc., Seoul, Korea) to an FTP server to continuously operate the system for approximately 3 months in the summer were acquired. Subsequently, the real-time data were transferred to build a database for the system. Moreover, it was configured to obtain power steadily from a solar cell on the exterior and the internal battery pack simultaneously (Figure 3a,b). The acoustic sensor unit was fixed and operated on the surface because the marine characteristics of HABs are concentrated on the surface during the daytime. To prevent noise caused by biofouling, the sensor surface was periodically cleaned using a hydro-wiper, and copper tape was attached to the side of the sensor.

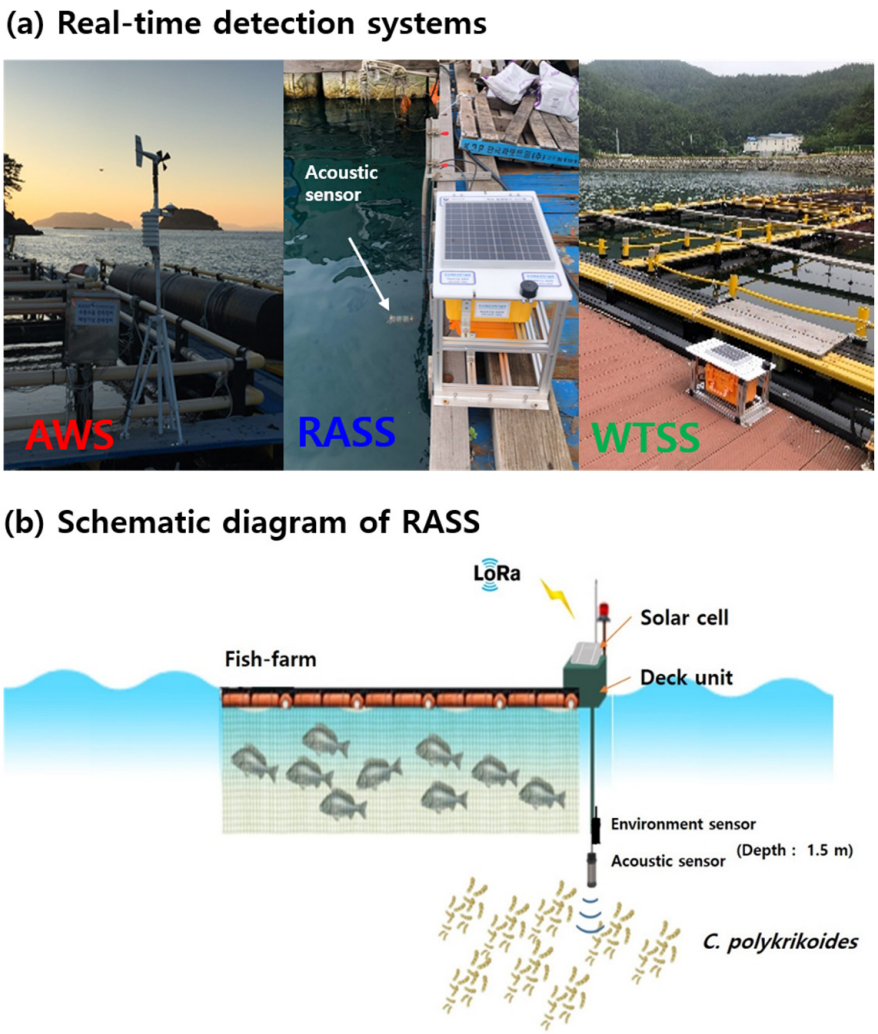

Figure 3. (**a**) Examples of real-time detection systems using the automatic weather system (AWS), red tide acoustic sensing system (RASS), and water temperature sensing system (WTSS); and (**b**) schematic of the RASS at a fish farm.

RASS detects HABs by acoustic sensing and measures the water temperature and salinity using a CT sensor (3919A, Aanderaa Inc., Bergen, Norway); however, some RASS stations are measured using various marine environmental data, such as water temperature, salinity, Chl-a, dissolved oxygen (DO), and pH (percentage of hydrogen ions) using a complex water-quality monitoring sensor (YSI EXO2; YSI Inc., Yellow Springs, OH, USA).

The AWS, which measured the air temperature, solar radiation, wind speed, and wind direction data for real-time marine meteorological observations, and the WTSS, which measured the water temperature and water pressure data, were simultaneously operated. The AWS and WTSS also transmitted data every 10 min to the FTP server via LoRa communication to build a database. The acquired data were checked in real time with those from the visualization system (Figure 3a).

The surface layer of the Chl-a data from GOCI, provided by the Korea Institute of Ocean Science & Technology (KIOST), was used for ocean satellite data. The Chl-a data were generated only for the southern coast, the area of interest, using techniques such as stray light deviation correction, atmospheric correction, and masking area minimization. We calculated the optimal Chl-a concentration for HAB detection using the red-to-blue ratio (RBR) technique, an algorithm optimized for HAB detection [31]. For satellite Chl-a data limited to daytime, image data with a 500 m $\times$ 500 m resolution were generated once

every hour and transmitted to the server. The satellite Chl-a data were acquired eight times a day during the daytime; these were synthesized in the data once daily.

2.2.3. Prediction System

HAB occurrence prediction and migration–diffusion models have been developed in many oceans. To improve the accuracy of HAB occurrence, movement, and diffusion prediction, the marine environment and ocean-current information of KOOS developed by KIOST were used as input data [32].

This prediction system predicts marine meteorological factors such as wind and atmospheric pressure. It generates marine environmental information on waves, tides, currents, ocean currents, water temperature, and salinity at a depth of 1 m at intervals of 1 h from the present to the next 72 h (3 days). However, building a model with a relatively high resolution is necessary, considering the phenomena of HAB movement and diffusion along the ocean current on the coast. Therefore, the KOOS model data were produced by establishing resolutions of 300 m for the entire southern coast and 150 m for the Tongyeong, Yeosu, and Geoje sites, the areas of interest. The data were predicted for 72 h (3 days), produced once a day, and sent to the server.

The HAB occurrence prediction model used marine meteorological and environmental data produced by the KOOS model of surface and observational data from a real-time HAB detection system, considering the characteristics of HABs concentrated on the surface during the daytime. In addition, long short-term memory (LSTM), a deep learning model, was employed, and the location and population data provided daily by NIFS through OpenAPI were used in the HAB information system (Figure 2) [5,33]. The data from 2000 to 2015 were converted into spatial data by georeferencing, using HAB occurrence data provided by NIFS based on GIS to train the model. The central coordinates were extracted from the converted HAB spatial data and used as HAB location information. The coordinates of HABs that occurred after 2016 were determined at the occurrence location using a differential global positioning system (DGPS). Among the data sampled, noise was added to the instances of occurrence to expand and balance the data, and learning was performed, because there are more cases of HAB non-occurrence than occurrence. The model resolution was set to 5 km, and the presence of the final HAB was determined based on a 50% probability. The model considered occurrence or non-occurrence if the probability was greater or less than 50%, respectively. These data predicted HAB occurrence after 3 days, and the data from the Tongyeong, Yeosu, and Geoje sites were produced as individual files, one per day, and sent to the server.

The HAB movement and diffusion prediction model is considerably influenced by the results of the marine environment and current velocity data because the model depends on the marine environment. *C. polykrikoides* information was generated as spatial data by extracting the sampling data provided daily by OpenAPI from the HAB information system of NIFS. The occurrence of the initial HAB particles was predicted using the concentration information provided in the HAB data. A model of movement and diffusion along ocean currents based on the KOOS data was built by applying a growth rate model for *C. polykrikoides*, a biological factor proposed by Cho et al. [34]. The resolution of the migration and diffusion prediction models was set to 300 m. The levels were classified according to the number of individuals, with less than 10 cells/mL classified as level 0, indicating no HAB; 10–100 cells/mL classified as level 1, indicating a preliminary caution for HAB; 100–1000 cells/mL classified as level 2, indicating a notice for HAB; and 1000 cells/mL or more classified as level 3, meaning a warning for HAB. The model data included forecast data from the present day to 72 h later, which were produced once daily and sent to the server.

2.2.4. Additional Data

The NIFS institutions provided information on the *C. polykrikoides* population and GPS coordinates of its occurrences once a day [5]. These data are available in the form of a *.netcdf file in OpenAPI format, which is provided daily. The HAB information acquired from NIFS is an input parameter in the occurrence model and the movement and diffusion model. It is displayed on the visualization screen within the integrated information system.

Additionally, information on *C. polykrikoides* occurrences is provided once a day in the form of a *.csv file through HAB information obtained from an in-house application. These data are used for basic reference purposes.

2.2.5. Integrated Information System

After storing the acquired data on a server, the integrated information system provides visual HAB detection and prediction information to public institutions such as research institutes, fishing villages, fishermen, and public agencies. For this purpose, an integrated HAB data storage server provided through OpenAPI, a public service capable of FTP file transfer, was built to store and share the detected and predicted data in real time [5]. Subsequently, people accessed the information system to detect and predict data.

A web-based visualization system was developed to display real-time detection and prediction data. An exhibition monitoring system was established based on a regional GIS, graphs, and text for user identification and convenience. The integrated visualization system mainly checks the data by changing to the GIS-based South Sea, Yeosu, and Tongyeong/Geoje sites. In addition, the detected and predicted data can be confirmed using a visualization system through various functions such as real-time detection information, prediction information, time-variation detection information, and data searches for each site.

2.2.6. Field Application of Integrated HAB Detection and Prediction System

The KORED system was operational in oceans to monitor HAB occurrences during the summer seasons (July–September) from 2017 to 2019. According to the annual plan, the system was utilized in the Tongyeong sites in 2017, both Tongyeong and Yeosu sites in 2018, and finally in the Tongyeong, Yeosu, and Geoje sites in 2019. However, in 2017, no HABs were reported in these Korean waters, and in 2018, they occurred only on a small scale in Tongyeong and Yeosu. This study focused solely on the data collected during the summer of 2019 when HABs occurred multiple times in the South Sea of Korea.

3. Results and Discussion

3.1. Real-Time HAB Detection System

3.1.1. RRL Validation from *C. polykrikoides* Population

The measurement of HAB (*C. polykrikoides*) populations and relatively received level (RRL) values in the field to calibrate the acoustic sensor indicated a good correlation, with RRL increasing as the number of *C. polykrikoides* populations increased (Figure 4a). Operating multiple RASSs at each site, most of the acoustic signals recorded were at the non-HAB level. However, signals indicating HAB caution or warning were recorded at some stations. The RRL values obtained from the beginning of July to the end of September at a specific station at the Tongyeong site ranged from 0 to 9 dB, which could be interpreted as the absence of HAB from all operating dates (Figure 4b). However, the RRL values obtained at a specific station in the Geoje area indicated the absence of HAB from early July to mid-August and a HAB caution or warning from late August to September (Figure 4c). The RRL value was relatively low in the morning and relatively high in the afternoon, confirming the effect of the vertical movement of phytoplankton. These data were consistent with those provided by the HAB information system of NIFS.

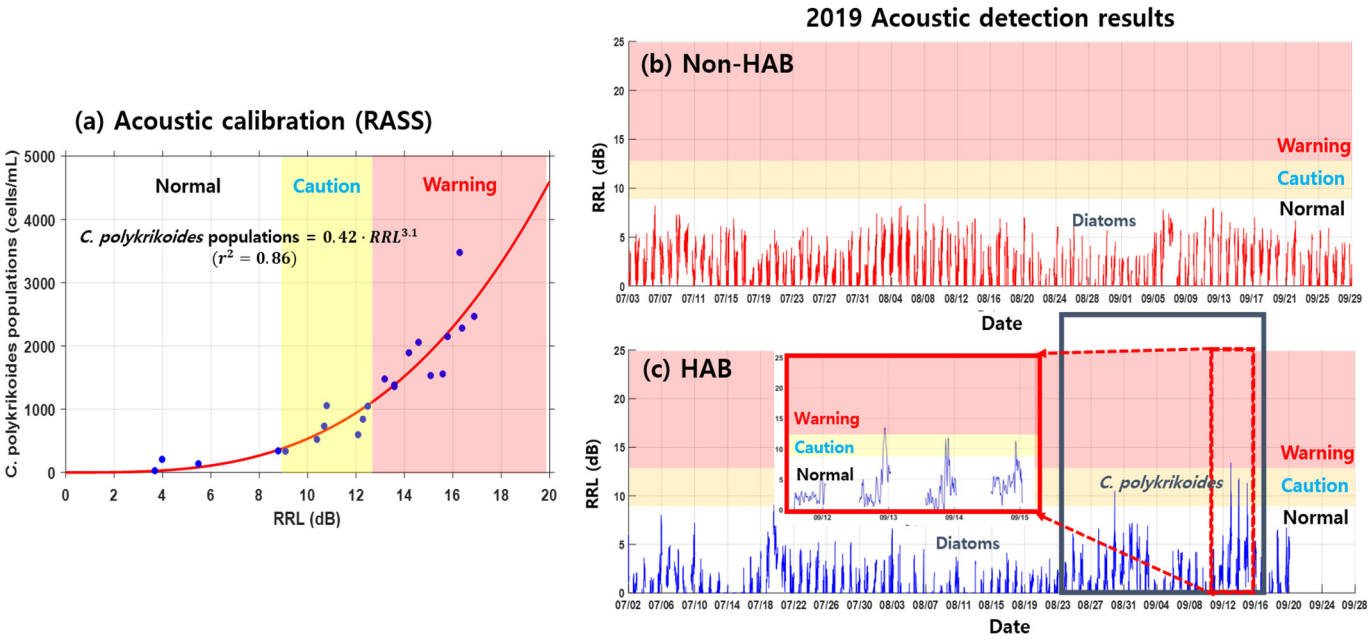

Figure 4. (**a**) Relatively received level (RRL) regression curve versus *C. polykrikoides* population. The results of the acoustic data of time series using the RASS; (**b**) non-HAB; and (**c**) HAB environments.

3.1.2. Operation of Detection System

Data obtained by installing and operating RASS, AWS, and WTSS stations (refer to 2.1 Study area) were confirmed in real time through a visualization system. In particular, acoustic signals caused by HABs were confirmed in some waters of Tongyeong and Yeosu during the summer. The Chl-a RBR data acquired over 3 months in summer through ocean observation satellites indicated almost 18 clear days with some clouds. This confirmed that the Chl-a concentrations were high values of more than 20 mg/m^3 in Yeosu, Tongyeong, and some ocean areas of Geoje, thus verifying the HAB distribution information over a wide area. Sampling analysis, genetic analysis, and optical detection using a camera were also performed to detect HABs rapidly. For sampling analysis, the sampling sites were observed at the Tongyeong, Geoje, and Yeosu sites to verify the HAB prediction models in the RASS site. The results were used to verify and evaluate the accuracy of the HAB occurrence, migration, and diffusion prediction models. Gene-based HAB organism real-time observation equipment using qPCR and gene observation and analysis was deployed simultaneously upon sampling from the Tongyeong, Geoje, and Yeosu sites. Results of the comparative study of the sampling and genetic data were similar (up to 1000 cells/mL, HAB warning level), confirming the feasibility of the rapid genetic diagnosis of field samples. Moreover, a portable optical detection module capable of photographing HAB species was developed and applied, and the acquired images were transmitted to researchers to rapidly detect HABs. A method that can rapidly determine the HAB species composition in the field in real time was applied to the integrated system.

3.2. HAB Prediction System

3.2.1. Operation of KOOS Model

Before operating the HAB prediction system to develop the KOOS model, the model results, ocean current speed, water temperature, Chl-a values, etc., measured in the ocean area were compared and analyzed. In particular, a comparison with the surface flowrate value measured by the buoy of Korea Hydrographic and Oceanographic Agency (KHOA) to verify the current or flowrate value, which is important for HAB movement and diffusion, indicated that the ocean current and current velocity model values of KOOS reproduced the direction well, compared with the actual values along the southern coast. However, because the observation buoy was positioned in the open ocean rather than the coast,

which is the focal station of HABs, verification of the conditions in the coastal region was constrained. The observed and predicted surface ocean current speed at 1 h intervals were compared, showing that the overall trend was reproduced but the small-scale residual component could not be reproduced. In addition, the results were compared after harmonic decomposition of each data, and although there was a difference in absolute size in both east-west and south-north components, the directionality was well reproduced. However, the overall direction was reproduced, and data assimilation was performed based on actual data to enhance the accuracy of the KOOS model. The model data produced values for predicting marine weather and marine environment information at 1 h intervals from the present to 72 h later. The data produced were uploaded to the FTP server as files for the oceanic meteorological and environmental factors for each ocean (Yeosu, Tongyeong, and Geoje). The visualization system displayed ocean-current information at 1 h intervals.

3.2.2. Evaluation of Prediction Model

The accuracy of the HAB prediction model was evaluated to verify its effectiveness. The accuracy was compared and analyzed using the data of 134 *C. polykrikoides* individuals obtained through 10 field surveys of net sampling conducted from August to September 2019. Field surveys were conducted at 22 stations from September 2 to 4 in the Yeosu, Tongyeong, and Geoje sites. Overall, in its early stage, HAB occurrence was predicted only in the western coastal areas of Yeosu sites; however, the diffusion range of the grid predicted a pattern similar to that shown by the actual diffusion range of HABs. Thus, the accuracy obtained by comparing 134 measured and predicted data values in 2019 was approximately 85%, confirming the usefulness and effectiveness of the model. The HAB prediction model predicted occurrence after 72 h from the present and produced data to predict the occurrence probability for each grid set in the sites. The visualization system displayed the probability of occurrence at 1-day intervals.

3.2.3. Evaluation of Movement and Diffusion Model

To assess the accuracy of the HAB movement and diffusion model, the predicted data were compared with and verified using data obtained through ocean sampling. The accuracy was determined by comparing the predicted values from the mobile diffusion model with the population of *C. polykrikoides* sampled from 22 stations across a wide area. The evaluation method proposed by Stumpf et al. [35] was employed for this purpose. An accurate KOOS model was utilized, and the evaluation range was limited to 10 km owing to the presence of many small islands with a radius of less than 10 km in the study area and the complicated coastal topography. The model was applied in a way that allowed the spatial error for each grid to be evaluated, assigning an 80% weight to adjacent grids within 5 km. Accordingly, the accuracy values are modified and presented as a method of assigning weights to adjacent grids. Even if the evaluation grid was set to within 10 km, higher accuracy is considered necessary for the effectiveness of the prediction, considering the geographical characteristics of many small islands and complex coastlines. The accuracy was assessed based on the model's prediction results at 12:00 on September 2 and 12:00 on September 4, 48 h later. The results from the sampling data are presented in Figure 5.

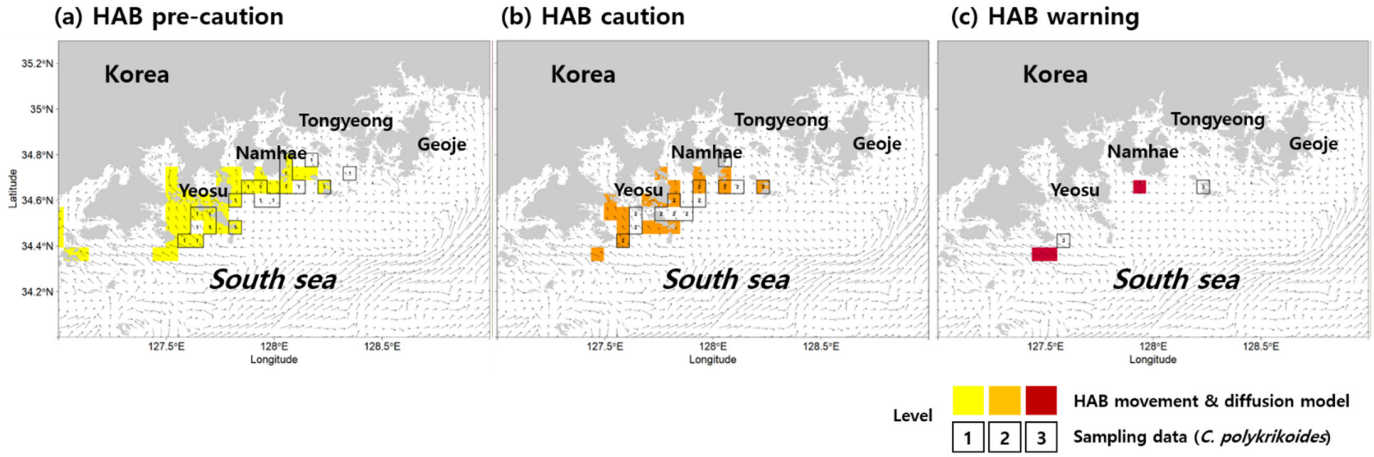

Figure 5. Accuracy evaluations from the HAB movement diffusion model (color boxes) and sampling data of *C. polykrikoides* (black number boxes) at: (**a**) 1 level (HAB pre-caution stage): 10–100 cells/mL; (**b**) 2 level (HAB caution stage): 100–1000 cells/mL; and (**c**) 3 level (HAB warning stage): more than 1000 cells/mL.

In Figure 5, the yellow, orange, and red boxes represent the model's prediction results for each stage. The boxes indicated by black numbers contain information on the population of *C. polykrikoides* at each location, as determined by microscopic analysis after sampling. The accuracy of the HAB movement and diffusion model was determined to be 89% and 87% at HAB pre-caution and caution levels 1 and 2, respectively. Additionally, the grid prediction accuracy at HAB warning level 3 was 40% (Figure 5a–c). Multiple accuracy evaluations yielded an average accuracy of approximately 70%, confirming the reliability and usefulness of the HAB movement and diffusion models within a resolution range of 5–10 km. However, the accuracy of the analysis results was compromised owing to the infrequent occurrence of high-concentration HABs of level 3 or higher in the sampling data. Nevertheless, the predicted locations of HABs were similar.

In particular, the prediction of the occurrence of high-density HABs caused by growth or accumulation was insufficient. At the HAB pre-caution and caution levels, the accuracy was mostly similar, but the warning level was sampled only twice, the prediction was less accurate at one point, and one point occurred in the immediate area; therefore, the accuracy was evaluated as half. The accuracy of the HAB movement and diffusion model can be improved if HAB data are provided more precisely in the limited areas of the Tongyeong, Geoje, and Yeosu oceans. Overall, the HAB particles moved and spread based on the ocean-current level, according to the grid set in the movement and diffusion model. In the visualization system, information on the location and concentration of HAB particles by ocean areas at 1 h intervals from the present to 72 h later was shown as a model that moved and spread along with the KOOS model.

3.3. Operation of Integrated Data Management and Visualization System

For all data acquired from the detection and prediction systems, a DB for each site/data was built on the server, and the data were uploaded and used when exhibited in the visualization system.

Figure 6 shows an sample screen of an HAB visualization system showing information obtained from each subsystem based on the GIS. The readability of the visualization system was improved by implementing a check box for each system on the left so that data points could be selected individually, or all acquired data could be checked simultaneously. Efficiency and usability were increased by implementing date/time so that data obtained on a desired date and at a particular time could be viewed at a glance. Figure 6 shows the data detected and predicted at the Tongyeong and Geoje sites using the past data search function.

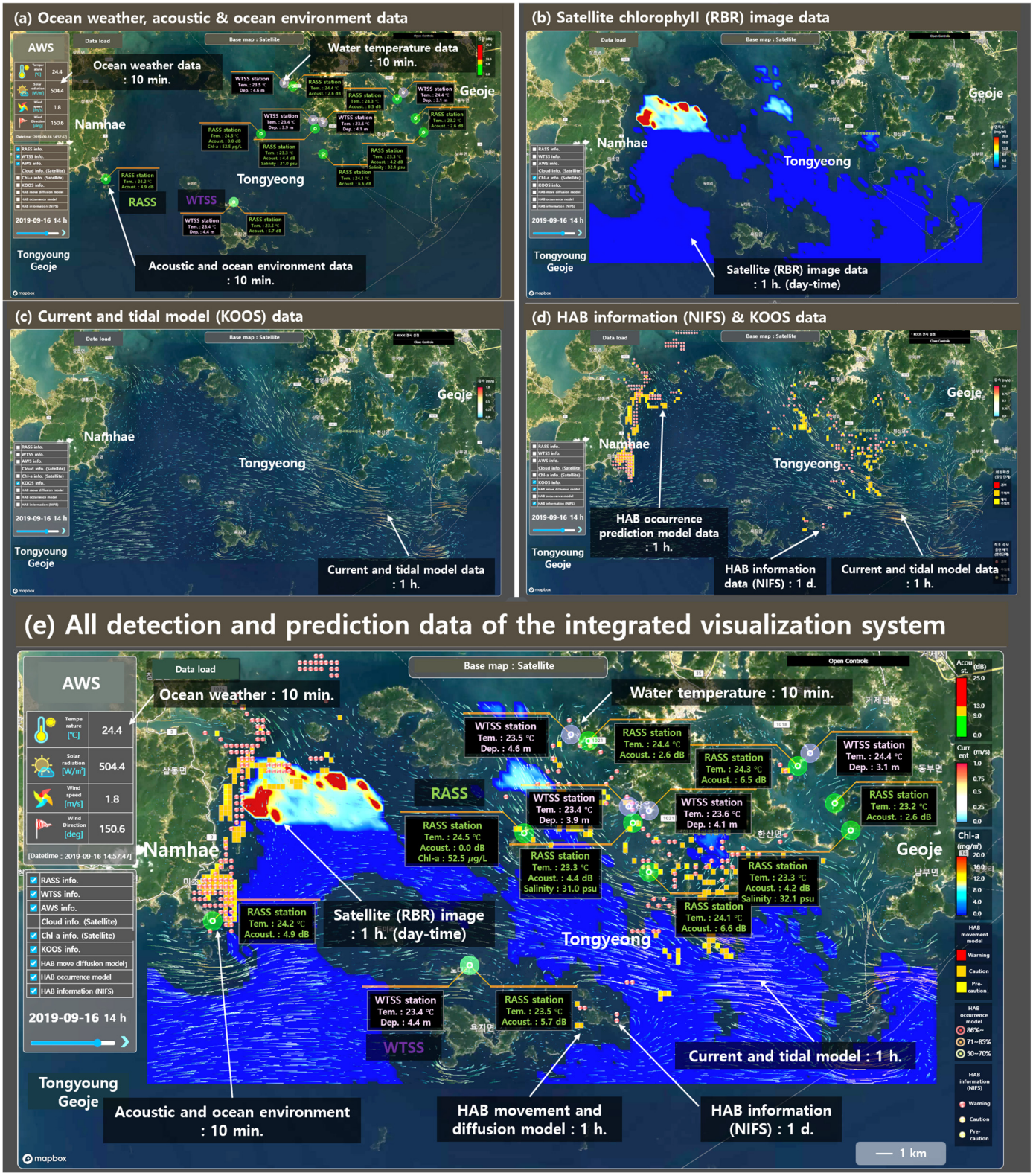

Figure 6. Examples of the visualization system at the Tongyoung and Geoje sites: (**a**) ocean weather, acoustic, and ocean environment data from AWS, RASS, and WTSS; (**b**) satellite chlorophyll (RBR) image data; (**c**) current and tidal model data; (**d**) HAB occurrence prediction model based on the HAB information (NIFS) data and the KOOS model data based on the geographic information system (GIS); and (**e**) all detection and prediction data of the integrated visualization.

Figure 6a shows the meteorological (AWS), acoustic, and marine environment (RASS); moreover, it shows water temperature (WTSS) data observed over a 10 min real-time period. Significantly, when a caution or warning level appears, the RASS icon is changed to yellow or red, corresponding to Figure 4. Figure 6b shows the satellite Chl-a concentration image data observed only during the daytime at 1 h intervals. It is updated eight times, and during the night, the RBR Chl-a image synthesized from eight sheets is displayed. The ocean-current model of KOOS predicted for 72 h at 1 h intervals is expressed as a current in Figure 6c. Because the current information is updated daily, it incorporates new 72 h current information 24 h after its initial update. The function of moving and spreading HAB particles according to the ocean current at an interval of 1 h was implemented. On September 16, HABs were predicted to be concentrated in the eastern area of Namhae Island, and the actual observation results were confirmed to be similar (Figure 6d).

All data detected and predicted at the Tongyeong and Geoje sites for each system subdivided in Figure 6e were integrated. All the data were simultaneously checked using a visualization system. The system was implemented and piloted to display real-time HAB detection and prediction data at the Tongyeong, Geoje, and Yeosu sites, which are wide and empirical oceans.

The water temperature, acoustic, and Chl-a data from measuring by RASS and WTSS are displayed as graphs for each station on the left-hand side of the fluctuation detection screen (Figure 7). Each entry of the real-time measurement data is displayed as a numerical value for each station in the table on the right. From August 28 to September 15, 2019, the signals caused by *C. polykrikoides* were detected via acoustic and Chl-a values at specific ocean sites. Thus, comprehensive HAB detection and prediction in real time is possible. The practicality and effectiveness of the system were confirmed by integrating various types of data and building a visualization system.

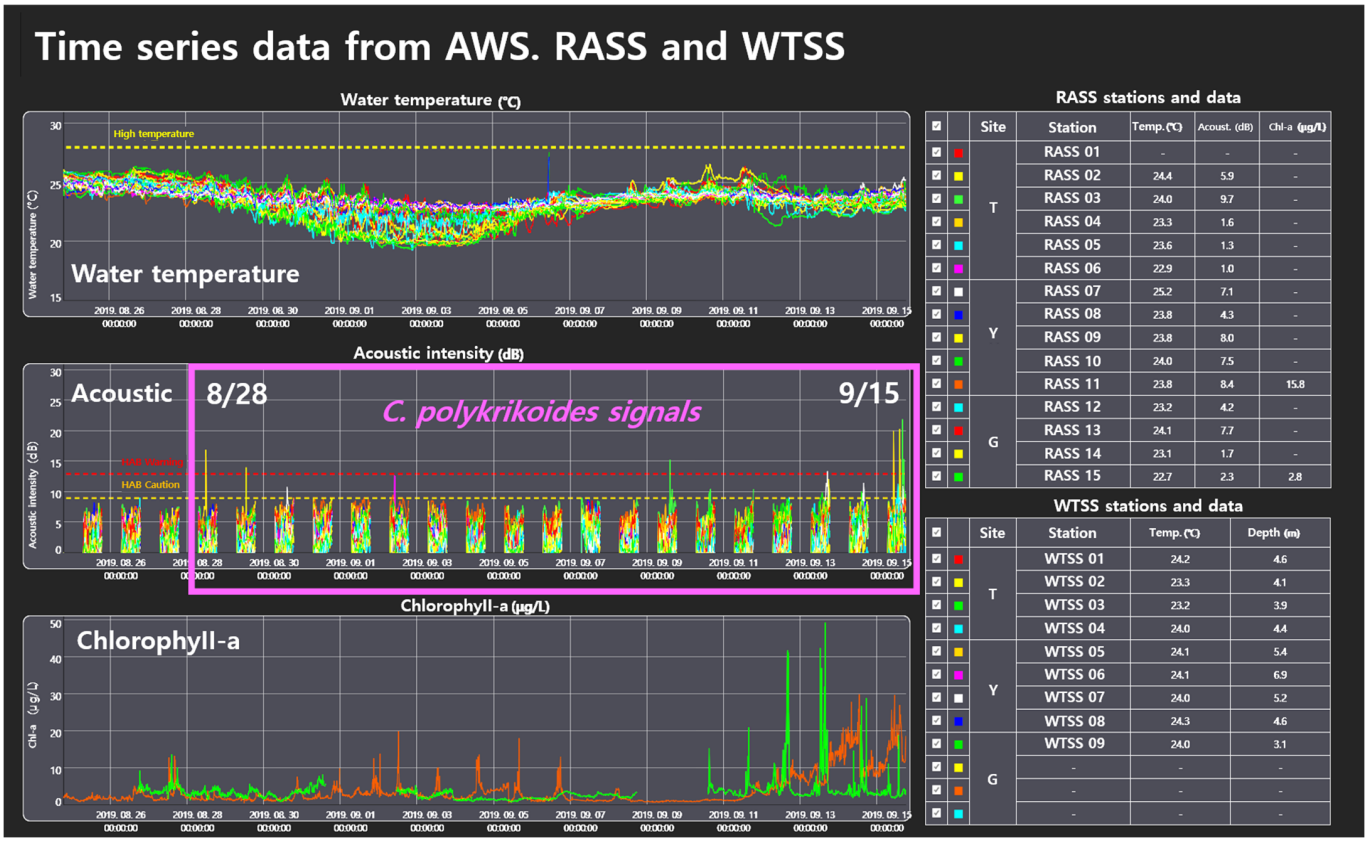

Figure 7. Examples from the time series graph and data table include water temperature, acoustic, and chlorophyll data from the AWS, RASS, and WTSS.

4. Conclusions

In this study, we developed an integrated system that combines various methods for HAB detection and prediction. One component of this system is the real-time HAB detection system, which incorporates ocean weather data, ocean parameters (such as water temperature, salinity, and Chl-a levels), satellite imagery, sampling, genetic analysis, and optical data. Another aspect involves prediction systems based on KOOS, HAB occurrence prediction, and HAB movement and diffusion models. Additionally, the system includes an integrated information system consisting of a data storage server, the FTP server, and the visualization system.

The integrated system was implemented on a trial basis from 2017 to 2019 at the Tongyeong, Yeosu, and Geoje sites in the southern coastal ocean, where HABs frequently occur during the summer. HAB information was compiled into a database and stored on a server. Consequently, a visualization system was made accessible to NIFS, local governments, fishermen, fishing villages, and relevant researchers. Notably, no HABs were detected in 2017. However, HABs were accurately detected and predicted in 2018 and 2019, confirming the practicality and effectiveness of the system.

While the integrated system was specifically piloted in the South Sea of Korea (Tongyeong, Yeosu, and Geoje sites), it can be applied to other oceans where HABs occurs frequently and the application of an integrated KORED system (HAB detection and prediction system) is needed. In terms of the future, the system has the potential to efficiently detect HABs in real time across a wide range, enabling more accurate predictions of HAB occurrence, movement, and diffusions through the practical application of integrated systems. There is also room to improve the accuracy of the HAB movement and diffusion model through future input data refinement. Implementing a more advanced integrated detection and prediction system in the field is anticipated in order to minimize the damage caused by irregular HAB occurrences every year.

Author Contributions: Conceptualization, D.K., S.W.J. and B.K.K.; methodology, H.K., S.W.J. and D.K.; software, H.K. and B.K.K.; formal analysis, H.K. and S.W.J.; investigation, H.K., S.W.J., S.H.B., J.-Y.C., H.-Y.C. and S.-J.L.; data curation, H.K., S.W.J., S.H.B., J.-Y.C., H.-Y.C. and S.-J.L.; visualization, H.K. and B.K.K.; project administration, D.K.; funding acquisition, D.K.; writing—original draft preparation, H.K. and D.K. All authors have read and agreed to the published version of the manuscript.

Funding: This research was supported by Korea Institute of Marine Science & Technology Promotion (KIMST), funded by the Ministry of Oceans and Fisheries, Korea (20170393).

Institutional Review Board Statement: Not applicable.

Informed Consent Statement: Not applicable.

Data Availability Statement: The data presented in this study are available upon request from the corresponding author. These data are not publicly available because they are part of an ongoing study.

Acknowledgments: We thank Junsu Kang, Young Kyun Lim, Hyun Jung Kim, Ki-Sub Lee, Mira Kim, Sungho Cho, Sung Kim, Wonkook Kim, Taek-Kyun Lee, Yeongwook Lee, and Seogil Jang for their assistance with the KORED system.

Conflicts of Interest: Author (Byoung Kweon Kim) was employed by the company (Syscore Inc.). The remaining authors declare that the research was conducted in the absence of any commercial or financial relationships that could be construed as a potential conflict of interest.

References

1. Rabalais, N.N.; Turner, R.E.; Diaz, R.J.; Justic, D. Global change and eutrophication of coastal waters. *ICES J. Mar. Sci.* **2009**, *66*, 1528–1537. [CrossRef]
2. Kim, H.G.; Jung, C.S.; Lim, W.A.; Lee, C.K.; Kim, S.Y.; Youn, S.H.; Cho, Y.C.; Lee, S.G. The spatio-temporal progress of *Cochlodinium polykrikoides* blooms in the coastal waters of Korea. *Kor. Soc. Fish. Aquat. Sci.* **2001**, *34*, 691–696. (In Korean)
3. Jeong, H.J.; Kim, S.K.; Kim, J.S.; Kim, S.T.; You, Y.D.; Yoon, J.Y. Growth and grazing rates of the heterotrophic dinoflagellate *Polykrikos kofoidii* on red-tide and toxic dinoflagellates. *J. Euk. Microb.* **2001**, *48*, 298–308. [CrossRef]

4. Seo, P.S.; Lee, S.J.; Kim, Y.; Lee, J.H.; Kim, H.G.; Lee, J.D. Axenic culture production and growth of a Dinoflagellate, *Cochlodinium polykrikoides*. *J. Korean Fish. Soc.* **1998**, *31*, 71–76. (In Korean)
5. NIFS. Standard of harmful algal blooms forecast in Korea. National Institute of Fisheries Science (NIFS). 2023. Available online: https://www.nifs.go.kr/red/main.red (accessed on 1 July 2023).
6. Kudela, R.M.; Gobler, C.J. Harmful dinoflagellate blooms caused by *Cochlodinium* sp. Global expansion and ecological strategies facilitating bloom formation. *Harmful Algae* **2011**, *4*, 71–86. [CrossRef]
7. Lauria, M.L.; Purdie, D.A.; Sharples, J. Contrasting phytoplankton distributions controlled by tidal turbulence in an estuary. *J. Mar. Syst.* **1999**, *21*, 189–197. [CrossRef]
8. Park, G.H.; Lee, K.; Koo, C.M.; Lee, H.W.; Lee, C.K.; Koo, J.S.; Lee, T.; Ahn, S.H.; Kim, H.G.; Park, B.K. A sulfur hexafluoride-based Lagrangian study on initiation and accumulation of the red tide *Cochlodinium polykrikoides* in southern coastal waters of Korea. *Limnol. Oceanogr.* **2005**, *50*, 578–586. [CrossRef]
9. Stumpf, R.P.; Culver, M.E.; Tester, P.A.; Tomlinson, M.; Kirkpatrick, G.J.; Pederson, B.A.; Truby, E.; Ransibrahmanakul, V.; Soracco, M. Monitoring Karenia brevis blooms in the Gulf of Mexico using satellite ocean color imagery and other data. *Harmful Algae* **2003**, *2*, 147–160. [CrossRef]
10. Ahn, Y.H.; Shanmugam, P.; Chang, K.I.; Moon, J.E.; Ryu, J.H. Spatial and temporal aspects of phytoplankton blooms in complex ecosystems off the Korean coast from satellite ocean color observations. *Ocean Sci. J.* **2005**, *40*, 67–78. [CrossRef]
11. Anglès, S.; Jordi, A.; Garcès, E.; Masó, M.; Basterretxea, G. High-resolution spatio-temporal distribution of a coastal phytoplankton bloom using laser in situ scattering and transmissometry (LISST). *Harmful Algae* **2008**, *7*, 808–816. [CrossRef]
12. Carvalho, G.A.; Minnetta, P.J.; Fleming, L.E.; Banzona, V.F.; Baringera, W. Satellite remote sensing of harmful algal blooms: A new multi-algorithm method for detecting the Florida Red Tide (*Karenia brevis*). *Harmful Algae* **2010**, *9*, 440–448. [CrossRef]
13. Gregg, W.W.; Casey, N.W. Global and regional evaluation of the SeaWiFS chlorophyll data set. *Remote Sens. Environ.* **2004**, *93*, 463–479. [CrossRef]
14. Vilas, L.G.; Spyrakos, E.; Palenzuela, J.M.T. Neural network estimation of chlorophyll a from MERIS full resolution data for the coastal waters of Galician rias (NW Spain). *Remote Sens. Environ.* **2011**, *115*, 524–535. [CrossRef]
15. Gitelson, A.A.; Dall'Olmo, G.; Moses, W.; Rundquist, D.C.; Barrow, T.; Fisher, T.R.; Gurlin, D.; Holz, J. A simple semi-analytical model for remote estimation of chlorophyll-a in turbid waters: Validation. *Remote Sens. Environ.* **2008**, *112*, 3582–3593. [CrossRef]
16. Park, M.-S.; Lee, S.; Ahn, J.-H.; Lee, S.-J.; Choi, J.-K.; Ryu, J.-H. Decadal Measurements of the First Geostationary Ocean Color Satellite (GOCI) Compared with MODIS and VIIRS Data. *Remote Sens.* **2022**, *14*, 72. [CrossRef]
17. Doucette, G.J.; Mikulski, C.M.; Jones, K.L.; King, K.L.; Greenfield, D.I.; Marin, R., III; Jensen, S.; Roman, B.; Elliott, C.T.; Scholin, C.A. Remote, subsurface detection of the algal toxin domoic acid onboard the Environmental Sample Processor: Assay development and field trials. *Harmful Algae* **2009**, *8*, 880–888. [CrossRef]
18. Greenfield, D.I.; Marin, R., III; Jensen, S.; Massion, E.; Roman, B.; Feldman, J.; Scholin, C.A. Application of environmental sample processor (ESP) methodology for quantifying Pseudo-nitzschia australis using ribosomal RNA-targeted probes in sandwich and fluorescent in situ hybridization formats. *Limnol. Oceanogr. Methods* **2006**, *4*, 426–435. [CrossRef]
19. Olson, R.J.; Sosik, H.M. A submersible imaging-in-flow instrument to analyze nano-and microplankton: Imaging FlowCytobot. *Limnol. Oceanogr. Methods* **2007**, *5*, 195–203. [CrossRef]
20. Kim, H.; Kang, D.; Jung, S.W. Development and application of an acoustic system for harmful algal blooms (HABs, red tide) detection using an ultrasonic digital sensor. *Ocean Sci J.* **2018**, *53*, 91–99. [CrossRef]
21. Kim, H.; Kang, D.; Jung, S.W.; Kim, M. High-frequency acoustic backscattering characteristics for acoustic detection of the red tide species *Akashiwo sanguinea* and *Alexandrium affine*. *J. Ocean. Limno.* **2019**, *37*, 1268–1276. [CrossRef]
22. Chen, C.S.; Gao, G.P.; Zhang, Y.; Beardsley, R.C.; Lai, Z.G.; Qi, J.H.; Lin, H.C. Circulation in the Arctic Ocean: Results from a high-resolution coupled ice-sea nested Global-FVCOM and Arctic-FVCOM system. *Prog. Oceanogr.* **2016**, *141*, 60–80. [CrossRef]
23. Huang, M.; Tian, Y. An Integrated Graphic Modeling System for Three-Dimensional Hydrodynamic and Water Quality Simulation in Lakes. *ISPRS Int. J. Geo-Inf.* **2019**, *8*, 18. [CrossRef]
24. Cruz, R.C.; Reis Costa, P.; Vinga, S.; Krippahl, L.; Lopes, M.B. A Review of Recent Machine Learning Advances for Forecasting Harmful Algal Blooms and Shellfish Contamination. *J. Mar. Sci. Eng.* **2021**, *9*, 283. [CrossRef]
25. Tian, Y.; Huang, M. An Integrated Web-Based System for the Monitoring and Forecasting of Coastal Harmful Algae Blooms: Application to Shenzhen City, China. *J. Mar. Sci. Eng.* **2019**, *7*, 314. [CrossRef]
26. Lee, C.K.; Park, T.G.; Park, Y.T.; Lim, W.A. Monitoring and trends in harmful algal blooms and red tides in Korean coastal waters, with emphasis on *Cochlodinium polykrikoides*. *Harmful Algae* **2013**, *30*, S3–S14. [CrossRef]
27. Park, T.G.; Lim, W.A.; Park, Y.T.; Lee, C.K.; Jeong, H.J. Economic impact, management and mitigation of red tides in Korea. *Harmful Algae* **2013**, *30*, S131–S143. [CrossRef]
28. Lim, W.A.; Lee, Y.S.; Lee, S.G. Characteristic of Environmental Factors Related to Outbreak and Decline of Cochlodinium polykrikoides Bloom in the southeast coastal waters of Korea, 2007. *J. Kor. Soc. Oceano.* **2008**, *7*, 68–77. (In Korean)
29. Lim, W.A.; Jung, C.S.; Lee, C.K.; Cho, Y.C.; Lee, S.G.; Kim, H.G.; Chung, I.K. The outbreak, maintenance, and decline of the red tide dominated by *Cochlodinium polykrikoides* in the coastal waters off southern Korea from August to October, 2000. *J. Kor. Soc. Oceano.* **2002**, *7*, 68–77. (In Korean)
30. Shim, J.-M.; Hwang, J.-D.; Jeong, C.-S.; Lee, Y.-H.; Jeon, K.-A.; Kwon, K.-Y. The influence of oceanic conditions on the occurrence of *Cochlodinium polykrikoides* blooms in the East Sea. *J. Env. Sci.* **2010**, *19*, 1385–1395. (In Korean) [CrossRef]

31. Noh, J.H.; Kim, W.; Son, S.H.; Ahn, J.H.; Park, Y.J. Remote quantification of *Cochlodinium polykrikoides* blooms occurring in the East Sea using geostationary ocean color imager (GOCI). *Harmful Algae* **2018**, *73*, 129–137. [CrossRef]
32. Park, K.S.; Heo, K.Y.; Jun, K.; Kwon, J.I.; Kim, J.; Choi, J.Y.; Cho, K.H.; Choi, B.J.; Seo, S.N.; Kim, Y.H.; et al. Development of the operational oceanographic system of Korea. *Ocean Sci. J.* **2015**, *50*, 353–369. [CrossRef]
33. Bak, S.H.; Jeong, M.J.; Hwang, D.H.; Enkhjargal, U.; Yoon, H.J. Study on *Cochlodinium polykrikoides* Red tide Prediction using Deep Neural Network under Imbalanced Data. *J. Kor. Ins. Electro. Com. Sci.* **2019**, *14*, 1161–1170. (In Korean) [CrossRef]
34. Cho, H.Y.; Park, K.S.; Kim, S. Global parameter estimation of the *Cochlodinium polykrikoides* model using bioassay data. *Acta Oceanol. Sin.* **2016**, *35*, 39–45. [CrossRef]
35. Stumpf, R.P.; Tomlinson, M.C.; Calkins, J.A.; Kirkpatrick, B.; Fisher, K.; Nierenberg, K.; Wynne, T.T. Skill assessment for an operational algal bloom forecast system. *J. Mar. Sys.* **2009**, *76*, 151. [CrossRef]